Available online at www.sciencedirect.com
ScienceDirect
Journal of Solid State Chemistry 181 (2008) 75–80
JOURNAL OF SOLID STATE CHEMISTRY
www.elsevier.com/locate/jssc

Efficient photoluminescence of Dy^{3+} at low concentrations in nanocrystalline ZrO_2

L.A. Diaz-Torres[a], E. De la Rosa[a,*], P. Salas[b], V.H. Romero[a], C. Angeles-Chávez[b]

[a]*Centro de Investigaciones en Optica, A.P. 1-948, Leon, Gto. 37150, Mexico*
[b]*Instituto Mexicano del Petroleo, L. Cárdenas 152, Mexico D.F. 07730, Mexico*

Received 11 May 2007; received in revised form 28 August 2007; accepted 24 September 2007
Available online 6 October 2007

Abstract

Nanocrystalline ZrO_2:Dy^{3+} were prepared by sol–gel and the structural and photoluminescence properties characterized. The crystallite size ranges from 20 to 50 nm and the crystalline phase is a mixture of tetragonal and monoclinic structure controlled by dopant concentration. Strong white light produced by the host emission band centered at ~460 nm and two strong Dy^{3+} emission bands, blue (488 nm) and yellow (580 nm), under direct excitation at 350 nm were observed. The highest efficiency was obtained for 0.5 mol% of Dy^{3+}. Emission is explained in terms of high asymmetry of the host suggesting that Dy^{3+} are substituted mainly into Zr^{4+} lattice sites at the crystallite surface. Luminescence quenching is explained in terms of cross-relaxation of intermediate Dy^{3+} levels.

Keywords: Dy^{3+}; ZrO_2; Photoluminescence; Nanocrystals; White light

1. Introduction

Rare earth ions have been playing an important role in modern lighting and display fields due to the abundant emission colors based on their 4*f*–4*f* or 5*d*–4*f* transitions [1]. In order to be excited efficiently, phosphors activated with rare earth ions should have a strong and broad absorption band in the UV or VUV region depending on the practical application situation. For example, the tricolor fluorescent lamp phosphors have a strong and broad absorption band around 254 nm (UV) to meet the irradiation from the discharge of low-pressure mercury vapor [1,2]. The visible luminescence of trivalent dysprosium Dy^{3+} mainly consists of narrow lines in the blue (470–500 nm, $^4F_{9/2} \rightarrow {}^6H_{15/2}$) and yellow ($^4F_{9/2} \rightarrow {}^6H_{13/2}$, 570–600 nm) wavelength region. The latter one belongs to the hypersensitive transition ($\Delta L = 2$, ΔJ=2), which is strongly influenced by the environment [3]. At a suitable yellow to blue intensity ratio, Dy^{3+} will emit white light. Thus, luminescent materials doped with Dy^{3+} may be used as potential two-band phosphors [4,5]. However, unlike the most frequently used Eu^{3+} and Tb^{3+} ions (in oxide hosts) that have allowed charge-transfer absorption band (CTB) or $4f^8$–$4f^7 5d$ absorption band in the UV region, respectively, the excitation spectrum of Dy^{3+} consists of only narrow *f*–*f* transition lines from 300 to 500 nm. Both the CTB and $4f^9$–$4f^8 5d$ excitation band of Dy^{3+} are located below 200 nm [6]. As a result, the photoluminescence (PL) of Dy^{3+} cannot be excited with 254 nm UV light, and the excitation can occur only by the *f*–*f* transitions with low oscillator strength (10^{-6}) due to their forbidden features by the parity selection rule [1]. This drawback of Dy^{3+} luminescence can be overcome by sensitization, such as host sensitization in YVO_4:Dy^{3+} [3] and ion sensitization in $Ca_2Gd_8(SiO_4)_6O_2$:Pb^{2+} Dy^{3+} [7].

Nanocrystalline ZrO_2 doped with different rare earths has been demonstrated to present suitable optical properties for photonics applications due to its enhanced luminescence properties [8–11], which in turn is due to nanosized effects. The very low stretching frequency of ZrO_2 (470 cm^{-1}) opens up the possibility of higher efficient luminescence of active ions incorporated into ZrO_2 matrix. Electrons confinement effect is not expected due to the localization of electrons in atomic orbitals of active ions. However, excitation dynamics is influenced by the nanoscopic

*Corresponding author.
E-mail address: elder@cio.mx (E. De la Rosa).

0022-4596/$ - see front matter © 2007 Published by Elsevier Inc.
doi:10.1016/j.jssc.2007.09.033

interaction and has been reported a dependence of the luminescence efficiency with particle size [12,13]. The interest on this new rare earth doped nanophosphor is to produce visible emission for application such as solid-state lighting, displays and new generation television screen. In particular, the development of UV LED open up new possibilities to obtain visible emission at any wavelength with the proper phosphor that must be developed [14]. Considering the promising optical properties of ZrO_2 and the spectral qualities of the Dy^{3+} UV excited emission, it is interesting to evaluate the luminescence properties of ZrO_2:Dy^{3+} for white light generation applications. Only few reports have been published on ZrO_2:Dy^{3+} nanocrystals. Recently, it has been reported the characterization of such kind of nanocrystals prepared for different methods. In those papers authors report that the PL depends on the crystalline phase and that the highest efficiency occur for samples doped at 2 mol% of Dy_2O_3 [15,16]. In this letter we present our study of the luminescence characterization of this nanophosphor prepared by sol–gel and its dependence on Dy^{3+} content. Here, PL depends strongly on Dy^{3+} concentration instead of crystalline phase. The highest efficiency was obtained for 0.5 mol% of Dy_2O_3 content contrary to results reported previously by others authors.

2. Experimental procedure

The samples were prepared by using the sol–gel method [17]. Undoped ZrO_2 was obtained by mixing zirconium *n*-propoxide as precursor in a solution of ethanol, nitric and hydrochloric acid at room temperature and vigorous stirring according to the molar rate 1:20:0.1:0.3, respectively. ZrO_2:Dy^{3+} samples were prepared by adding different molar concentrations (0.1, 0.5, 1.0 and 2.0 mol%) of Dy_2O_3 using dysprosium nitrates, corresponding to Zr/Dy molar ratios of 1:0.001, 1:0.005, 1:.01, and 1:0.02, respectively. CO_2-free distilled water in the molar ratio of 1:4 was added dropwise to manipulate the hydrolysis process. After gelation, the samples were aged at 120 °C for 12 h followed by calcinations at 400 °C for 5 h. Temperature was raised to 1000 °C at a rate of 5 °C/min; as soon as the temperature was reached, sample was retired from the furnace.

The crystalline structure and crystallite size of samples were investigated by X-ray diffraction (XRD) using a Siemens D-500 equipment with $\lambda = 1.5405$ Å, scanning in the 15–80° 2θ range with 0.05° increments and 3 s swept. The morphology and crystallite size was analyzed in a field-emission electron microscope JEM-2200FS operating at 200 kV. The microscope is equipped with an ultra high resolution (UHR) configuration ($C_s = 0.5$ mm; $C_c =$ 1.1 mm; point-to-point resolution, 0.19 nm).

Both fluorescence excitation and emission spectra are recorded on an Acton Research modular 2300 spectrofluorometer. The excitation source is a 75 W Xenon lamp. The spectral resolution of the spectrofluorometer was 1 nm.

3. Results and discussions

The crystalline phase of ZrO_2:Dy^{3+} nanocrystals is a mix of monoclinic (*m*) and tetragonal (*t*) phase being the phase composition determined by the ion concentration, see Fig. 1. The diffraction pattern for the 0.1 mol% Dy_2O_3 doped sample was dominated by the $(-1,1,1)_m$ and $(1,1,1)_m$ reflections characteristic of the monoclinic phase. The $(0,1,1)_t$ reflection is characteristic of the metastable tetragonal phase and was much more smaller than monoclinic reflections for dopant concentration lower than 1 mol%. This indicates the dominant presence of the monoclinic phase in relation to the tetragonal phase. As the Dy^{3+} ion concentration increases the monoclinic peaks diminishes whereas the tetragonal peak increases, being dominant for the 2.0 mol% Dy_2O_3 content. This behavior in the phase composition is consistent with previous reports on rare earth stabilization of different ZrO_2 crystalline phases [17,18]. The phase composition, average crystallite size and lattice parameters of both the monoclinic and tetragonal structures were calculated for 0.5 and 2.0 mol% of Dy_2O_3 doped samples by using the Rietveld method [19], and listed in Table 1. The major content of the tetragonal phase was 52.8 wt% for the sample with 2.0 mol% Dy_2O_3 whereas for the sample with 0.5 mol% Dy_2O_3 the tetragonal phase content was only 8.7%. This indicates the enhancing effect of the impurity addition on the stability of the tetragonal phase up to 1000 °C. Average crystallite sizes of 22.8 and 40.0 nm for 0.5 and 2.0 mol% Dy_2O_3 content, respectively, were estimated from the tetragonal phase. And crystallite sizes of 47.2 and 36.4 nm for 0.5 and

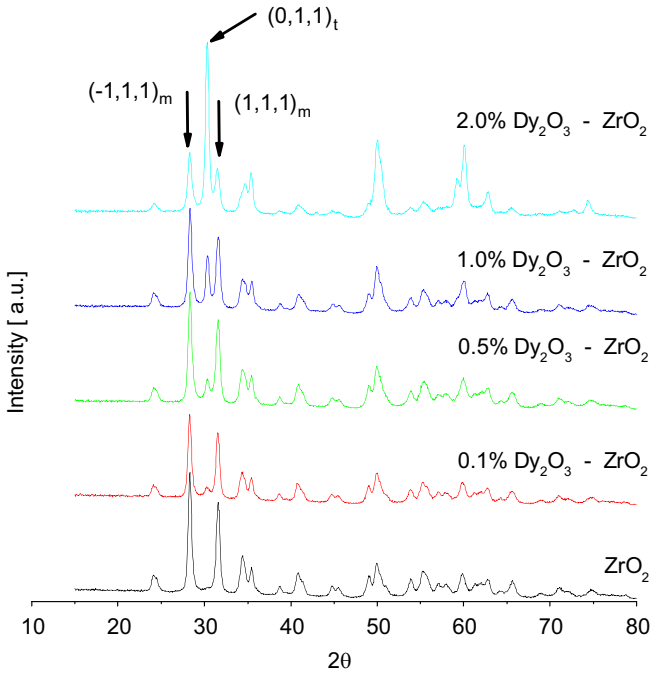

Fig. 1. XRD patterns for undoped and Dy^{3+} doped nanocrystals. Reflection peaks are denoted according to JCPDS 37-1484 (monoclinic) and JCPDS 50-1089 (tetragonal).

Table 1
Phase composition, crystallite size and lattice parameter obtained from Rietveld refinement

Dy_2O_3 (mol%)	Phase composition (wt% ±4%)	Lattice parameters (A ±0.1%)				Cell volume (A^3)	Crystallite size (nm ±2%)
		a_o	b_o	c_o	β		
0.5	Tetragonal (8.7)	3.598	3.598	5.181		67.09	22.8
	Monoclinic (91.3)	5.149	5.202	5.314	99.02	142.37	47.2
2.0	Tetragonal (52.8)	3.598	3.598	5.183		67.13	40.0
	Monoclinic (47.2)	5.151	5.204	5.314	98.9	142.50	36.4

2.0 mol% Dy_2O_3 content, respectively, were estimated for the monoclinic phase. Both crystallite size and phase composition obtained from XRD results and Rietveld refinement analysis are in agreement with results obtained from TEM and HRTEM images. The particle size measured from TEM ranges between 20 and 50 nm and all these nanoparticles are well faceted, see Fig. 2a. The change in lattice parameters is induced by the difference of ion size of Dy^{3+} (1.03 Å) and Zr^{4+} (0.84 Å). Such changes confirm that Dy^{3+} is substituting Zr^{4+} ion. The valence difference of the substituted cations requires charge compensation that leads to small local distortions of the crystalline lattices, with an overall loss of symmetry in both crystalline phases. Up to the annealing temperature of the samples there was not observed Dy_2O_3 crystalline phase in the bulk or surface of the zirconia nanoparticles suggesting that the Dy^{3+} atoms remain within the crystallite lattices of both phases. The HRTEM images show the atomic resolution corresponding to the monoclinic zirconia phase in the [211] direction and tetragonal zirconia phase in the [100] direction, see Fig. 2b. From the HRTEM of both phases, there is no evidence of the presence of Dy_2O_3 crystalline phase on the nanoparticles, confirming that Dy^{3+} ions remain within the crystalline lattices.

The excitation spectrum in Fig. 3 is the scanning excited wavelength from 300 to 410 nm when the detection wavelength was set at 488 nm, for the sample with 0.5 mol% of Dy_2O_3 content. The excitation maxima for the 488 nm emission is located at 350 nm corresponding to the transition from the ground level $^6H_{15/2}$ to the hypersensitive level $^6P_{7/2}$, from where it relaxes nonradiatively to the $^4F_{9/2}$ metastable level. Three secondary excitation peaks at 326, 366, and 388 nm were assigned and correspond to the transitions from the ground level ($^6H_{15/2}\rightarrow{}^6P_{3/2}$), ($^6H_{15/2}\rightarrow{}^6P_{5/2}$), ($^6H_{15/2}\rightarrow{}^4F_{7/2}$), respectively. The general observed peaks distribution agrees with the reported structure distribution spectra for ZrO_2:Dy^{3+} nanocrystals [15]. Those broad bands indicate that the Dy^{3+} ions are substituted mainly at Zr^{4+} sites with high symmetry, that is, at the more symmetric eight-fold coordination sites of the Zr^{4+} cation within the tetragonal phase [15]. Thus, this excitation spectrum suggests that most of the Dy^{3+} ions are substituted within the tetragonal crystallites. The experimental results in Fig. 4 show the fluorescence emission from 400 to 650 nm of the five prepared samples annealed at 1000 °C, both undoped and

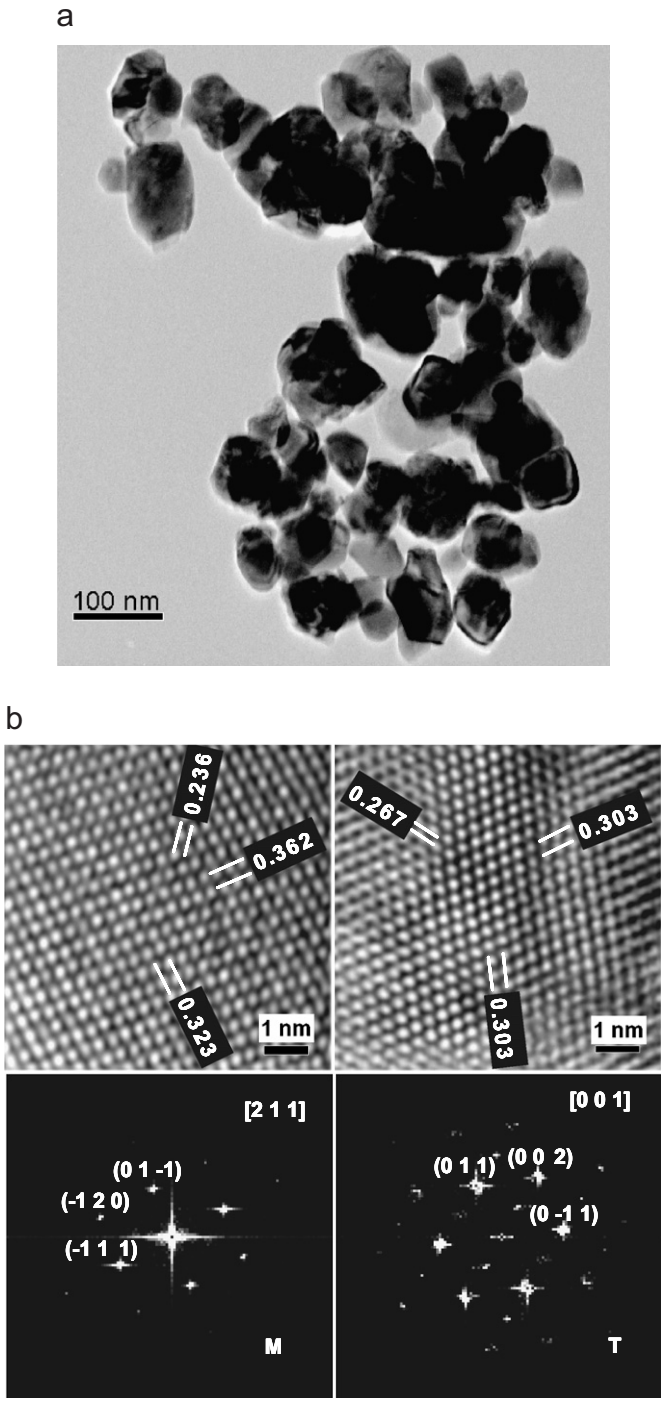

Fig. 2. (a) TEM, (b) HRTEM and FFT for Zr_2O_3:Dy^{3+} nanocrystal doped at 0.5 mol%.

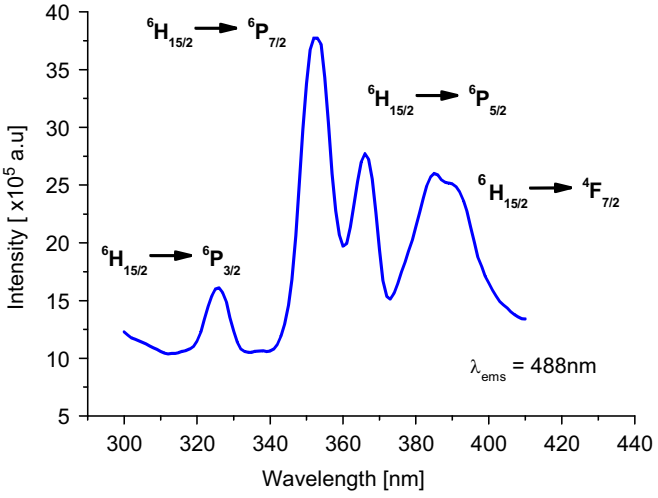

Fig. 3. Excitation spectrum of sample doped at 0.5 mol% of Dy^{3+}.

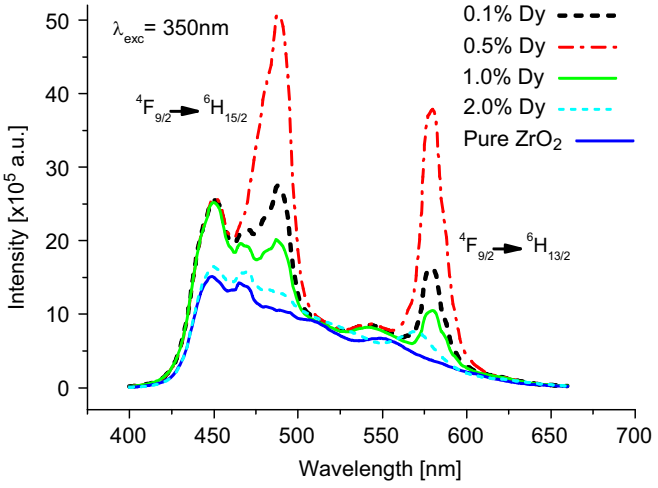

Fig. 4. Photoluminescence spectra of undoped and Dy^{3+} doped nanocrystals.

doped ZrO_2 under excitation at 350 nm. The broad emission band is dominated by two main peaks, the strongest one in the blue region centered at 488 nm ($^4F_{9/2} \rightarrow {}^6H_{15/2}$) and a less strong one in the yellow region centered at 580 nm ($^4F_{9/2} \rightarrow {}^6H_{13/2}$), both characteristic of Dy^{3+} in a solid solution [20]. Notice that the 2.0 mol% Dy_2O_3 doped sample had an emission almost indistinguishable from the undoped sample. Such behavior indicates that the Dy^{3+} luminescence was completely quenched for a 2.0 mol% content. It is also shown the emission of undoped ZrO_2 which has a broad emission band extending from 425 to 650 nm peaking around 460 nm [21]. The shape of the UV side of this emission band is defined by the transmittance of the filter used to stop the excitation wavelength. In this case, electrons promoted to the conductive band decay non radioactively to the recombination band associated to traps produced by the presence of defects [10]. From this metastable band electrons decay to the valence band producing the broad emission. All transition associated to signal emitted are described in the energy diagram from Fig. 5. It is also worth to notice that the host band actually corresponds to the baseline for the Dy^{3+} emission on the doped samples. Therefore, the luminescence of the doped system simply corresponds to the superposition of host plus the impurity emissions. This fact indicates that there is no energy transfer processes between the host and the Dy^{3+} ions in opposite of results reported by Fu et al. [15]. That difference might be due to the fact that in Ref. [15] high concentrations of Y^{3+} have been added as codopants in order to stabilize different crystalline phases, that in turn increases substantially the number of oxygen vacancies which on time act as sensitizers of Dy^{3+}. In that sense, the absence of energy transfer in our samples might be an indication of a reduced amount of oxygen vacancies.

One can observe that the highest emission corresponds to the 0.5 mol% Dy_2O_3 doped sample, which presents mainly the monoclinic structure. For all samples the emission is dominated by the magnetically allowed ($^4F_{9/2} \rightarrow {}^6H_{15/2}$) transition that hardly varies with variations of the crystal field strength around the Dy^{3+} ion. The ratio of the ($^4F_{9/2} \rightarrow {}^6H_{15/2}$) transition to the hypersensitive ($^4F_{9/2} \rightarrow {}^6H_{13/2}$) transition keeps an almost constant value of 1.28 ± 0.04 over the range of Dy^{3+} content. That indicates that in spite of considerable changes on phase content, the hypersensitive transition ($^4F_{9/2} \rightarrow {}^6H_{13/2}$) senses on average the same degree of asymmetry at the substituted Dy^{3+} sites. This leads to assume that in spite that the tetragonal content increases with Dy^{3+} concentration, a great amount of such tetragonal crystallites have distorted tetragonal cells and in consequence the Dy^{3+} ions on such crystallites continue to sense reduced local symmetry, that on turn lead to an increased luminescence emission. Loss of local symmetry is also induced by surface defects that in turn are a consequence of small crystallite size. These results suggest that Dy^{3+} ions could be distributed along the nanocrystals producing a gradient ion, being

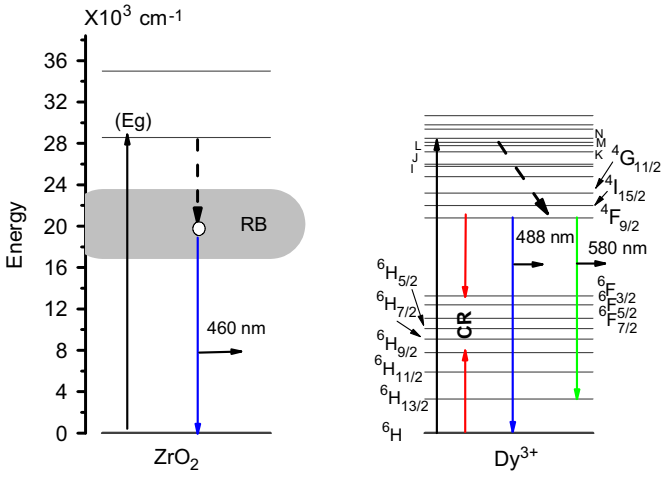

Fig. 5. Energy diagram indicating the transition involved in the visible emission.

accumulated in few planes in the surface substituted at some Zr^{4+} lattice sites. The absence of changes of hypersensitive transition is in opposite to results reported by Gu et al. [16] where they claim to observe changes in the blue to yellow bands ratio as the phase composition change. In addition, concentration quenching of the Dy^{3+} luminescence is observed as Dy^{3+} concentration increases over 0.5 mol% Dy_2O_3 content. Luminescence of the 2.0 mol% Dy_2O_3 doped sample is almost identical to the host luminescence. The most plausible explanation for such behavior is cross relaxation among Dy^{3+} pairs to the intermediate levels Dy^{3+} ($^6F_{3/2}$) and Dy^{3+} ($^6H_{9/2}$), from where the ions decay non radiatively or by IR emission, see energy diagram in Fig. 5 [22,23]. These quenching transitions are mainly Dy^{3+} ($^4F_{9/2}$) + Dy^{3+} ($^6H_{15/2}$) → Dy^{3+} ($^6F_{3/2}$) + Dy^{3+} ($^6H_{9/2}$). The quenching of the Luminescence is best observed on Fig. 6 where one can note the drastic reduction of the total emission from 0.5 mol% Dy_2O_3 to 2.0 mol% Dy_2O_3. Such behavior indicates that for nanocrystalline ZrO_2:Dy^{3+} the optimum concentration is around 0.5 mol% Dy_2O_3 content, which is to our knowledge the lowest concentration for maximum Dy^{3+} PL in a ceramic phosphor.

The spectral characteristics of this new phosphor make it a promising candidate for application on optical devices and solid-state lighting for general illumination purposes. Nanocrystalline ZrO_2:Dy^{3+} shows its main peak emissions in blue as well yellow spectral regions, and has a strong broad host emission band extending from 400 to 650 nm. Consequently, the emission color of nanocrystalline ZrO_2:Dy^{3+} is a white color tending slightly to yellowish. Inset in Fig. 6 shows the PL emission observed under excitation at 350 nm. It is important to consider the relatively strong emission observed in spite of the low excitation intensity coming from the spectrofluorometer with slits set at 5 μm. The CIE coordinates measured with a LS2000 Minolta colorimeter were $x = 0.36350$ and $y = 0.4077$. The color coordinates were verified with the help of a CIE chromaticity coordinates diagram confirming the yellowish white color shown in Fig. 6.

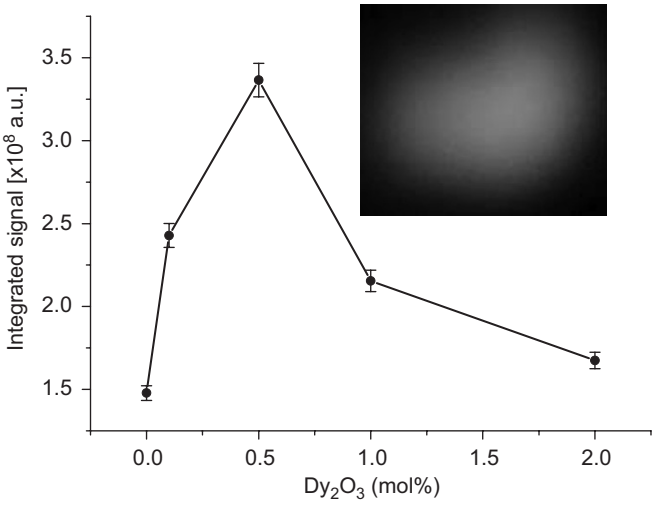

Fig. 6. Integrated photoluminescence as function of Dy^{3+} concentration. The inset shows a picture of white emission.

4. Conclusions

In summary, nanocrystalline ZrO_2:Dy^{3+} have been synthesized by sol–gel method and highly efficient yellowish white light emission at 0.5 mol% Dy_2O_3 was observed. Dy^{3+} concentration determines both luminescence properties and crystalline phase composition. Results suggest that nanocrystalline ZrO_2:Dy^{3+} (0.5%) is a promising phosphor candidate for white lighting applications. The strong quenching above 1.0 mol% content and the constant value of the ratio ($^4F_{9/2}$ → $^6H_{15/2}$)/($^4F_{9/2}$ → $^6H_{13/2}$) suggest that Dy^{3+} ions are distributed along the nanocrystal but mainly in few planes on the surface substituted at the Zr lattice sites.

Acknowledgments

This works was partially supported by CONACyT trough Grants 43168-F, 46971-F and scholarship for V.H. Romero. The help of Dr. R. A. Rodriguez in the color coordinate measurement is also acknowledged.

References

[1] G. Blasse, B.C. Grabmaier, Luminescent Materials, Springer, Berlin Heidelberg, 1994.
[2] C. Feldmann, T. Justel, C.R. Ronda, P.J. Schmidt, Adv. Funct. Mater. 13 (2003) 511.
[3] J.L. Sommerdijk, A. Bril, F.M.J.H. Hoex-Strik, Philips Res. Rep. 32 (1977) 149.
[4] Q. Su, Z. Pei, L. Chi, H. Zhang, F. Zou, J. Alloys Compds. 192 (1993) 25.
[5] Q. Su, Z. Pei, J. Lin, F. Xue, J. Alloys Compds. 225 (1995) 103.
[6] E. Loh, Phys. Rev. 147 (1966) 332.
[7] J. Lin Q. Su, J. Alloys Compds. 210 (1994) 159.
[8] A. Patra, C.S. Friend, R. Kapoor, P.N. Prasad, Appl. Phys. Lett. 83 (2003) 284.
[9] Z. Assefa, R.G. Haire, P.E. Raison, Spectrochim. Acta Part A 60 (2004) 89–95.
[10] E. De la Rosa-Cruz, L.A. Diaz-Torres, P. Salas, R.A. Rodríguez, G.A. Kumar, M.A. Meneses, J.F. Mosiño, J.M. Hernández, O. Barbosa-García, J. Appl. Phys. 94 (2003) 3509.
[11] P. Salas, C. Angeles, J.A. Montoya, E. De la Rosa, L.A. Díaz-Torres, A. Martínez, M.A. Romero-Romo, J. Morales, Opt. Mater. 27 (2005) 1295.
[12] P.K. Sharma, M.H. Jilavi, R. Nass, H. Schmidt, J. Lumin. 82 (1999) 187.
[13] R.S. Meltzer, W.M. Yen, H. Zheng, S.P. Feofilov, M.J. Dejneka, B. Tissue, H.B. Yuan, J. Lumin. 94–95 (2001) 217.
[14] R. Muller-Mach, G.O. Muller, M.R. Krames, T. Trottier, IEEE J. Sel. Topics Quantum Electron. 8 (2002) 339.
[15] X. Fu, S. Niu, H. Zhang, Q. Xin, Mater. Sci. Eng. B 129 (2006) 14.
[16] F. Gu, S.F. Wang, M.K. Lu, G.J. Zhou, S.W. Liu, D. Xu, D.R. Yuan, Chem. Phys. Lett. 380 (2003) 185.
[17] W. Córdova-Martínez, E. De la Rosa-Cruz, L.A. Díaz-Torres, P. Salas, A. Montoya, M. Avendaño, R.A. Rodríguez, O. Barbosa-García, Opt. Mater. 20 (2002) 263.

[18] M.K. Naskar, M. Chatterjee, D. Ganguli, Bull. Mater. Sci. 25 (5) (2002) 413.
[19] B.D. Cullity, Elements of X-ray Diffraction, second ed., Addison-Wesley, Reading, MA, 1978, pp. 102.
[20] G. Dominiak-Dzik, W. Ryba-Romanowski, M.N. Palatnikov, N.V. Sidorov, V.T. Kalinnikov, J. Mol. Struct. 704 (2004) 139.
[21] E. De la Rosa-Cruz, L.A. Diaz-Torres, P. Salas, V.M. Castaño, J.M. Hernandez, J. Phys. D: Appl. Phys. 34 (2001) L83–L86.
[22] W.Y. Shen, M.L. Pang, J. Lin, J. Fang, J. Electrochem. 152 (2) (2005) H25–H38.
[23] G. Tripathi, V.K. Rai, S.B. Rai, Spectrochim. Acta A 62 (2005) 1120–1124.